Chapter-2

Experimental Techniques

2.1 Overview

This chapter deals with experimental methods and characterization techniques utilized in the thesis dissertation. This chapter explains sample preparation, fabrication methods, characterization techniques, and their working principles in detail.

This chapter consists of three sections:

(1) Different synthesis and materials fabrication techniques are involved in sample preparation.

(2) Characterization techniques used for crystal structure analysis, thermal analysis, and electrical analysis.

(3) Data analysis tools such as X-ray Rietveld refinement, microstructural study, Electrochemical study, and impedance spectroscopy.

2.2 Synthesis Technique

Preparation of materials in the range of nano regime will be classified into two categories; top-down and bottom-up. The top-down process involves the reduction of bulk to nanoparticles such as ball milling and sputtering, etc. The bottom-up process is the building of nanomaterials from atom by atom or molecule by molecule. Chemical synthesis methods have significant advantages during the bottom-up process such as uniform size, shape, and distribution of nanomaterial can be obtained.

Morphology of the material plays a vital role in deciding the suitability of the electrode material in supercapacitor applications. To conceive excellent nanostructures, it is important to choose the appropriate methodology. Oxalate-based architectures can be engineered through various synthetic methods like the sol-gel route [1], hydrothermal approach [2], microwave-irradiation method [3], and co-precipitation technique [4], and so on [5]. Among

these methods, the co-precipitation approach is effective to fabricate materials with desired morphology with the porous network. Moreover, it is a process in which soluble compounds are further carried out of solution by precipitate it is a cost-effective method to build nanostructures. Furthermore, Aqueous solvents are used easily to prepare, and immediate product formation (within a short period), and uniform reaction within the species are the added merits of the coprecipitation methodology [6]. Homogeneous precipitation can be obtained via a process that involves the separation of the nucleation and growth of the nuclei. Two stages are involved in this process: (i) a short burst of nucleation when the concentration of the species reaches critical supersaturation and (ii) a slow growth of the nuclei by diffusion of the solutes to the surface of the crystal [7]. To obtain mono-dispersed nanoparticles, these two stages should ideally be separated, that is, nucleation should be avoided during the period of growth.

2.2.1 Coprecipitation synthesis route

Weighing of required compounds is the initial step. With the help of the electronic weighing machine, the weight of compounds gets measured with a proper stoichiometric ratio. Subsequently, deionized water as solvent has been taken into a beaker followed by the preparation of a homogeneous solution of cationic salt. Afterward, the anionic group has been added to the solution which further resulted in the precipitate of the compound. Moreover, filtration with help of filter paper accompanied with calcination of compound take place. Grinding will be done to reduce fine powder for application purposes.

Flow chart of the process:

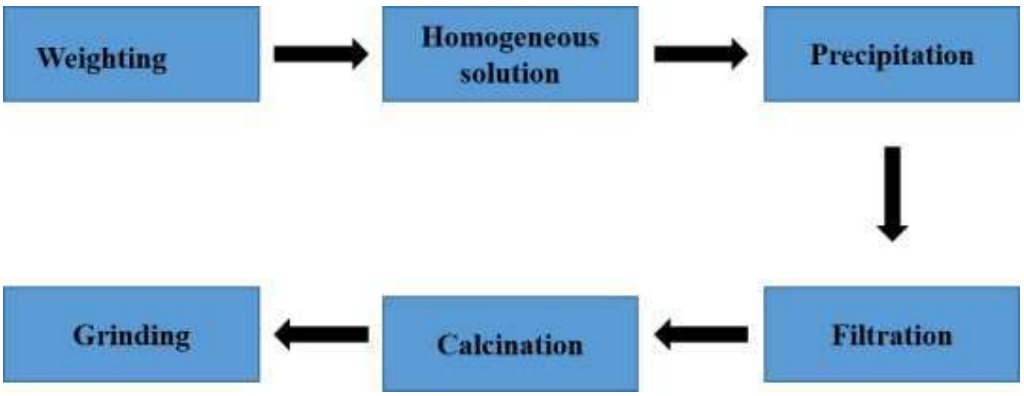

Figure 2.1 Flow Chart of synthesis process

2.3 Material Characterization Techniques

The following section describes the characterization techniques used during this work. The basics of each method are briefly described in the next section. Here are the main techniques listed.

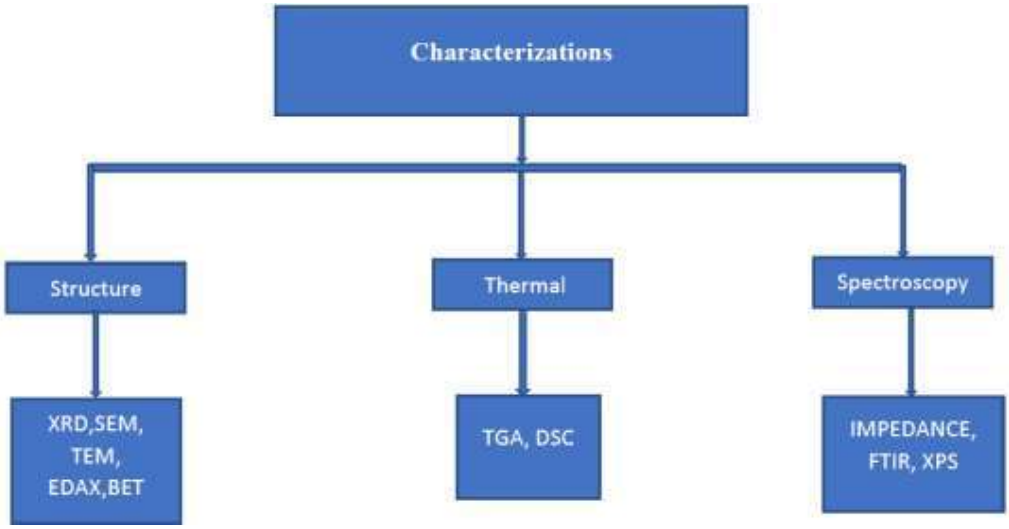

Figure 2.2 Characterization techniques used

2.3.1 Powder X-Ray Diffraction (XRD)

X-ray diffraction is an (XRD) powerful non-contact and non-destructive technique, making it ideal for structural studies. It uniquely identifies the crystalline phases present in the material. It measures the structural properties like phase composition, grain size, preferred orientation, strain state, defect structure, and epitaxy of these phases present in the compound. The intensities obtained from the XRD can provide quantitative and accurate information on the atomic arrangements at interfaces. Materials having a different composition of elements can be successfully identified with XRD. Still, they are very sensitive to the elements having large atomic numbers because the diffracted intensities are enormous compared to those with lower atomic numbers. It predicts the quantitative phase analysis and qualitative structural and microstructural analysis.

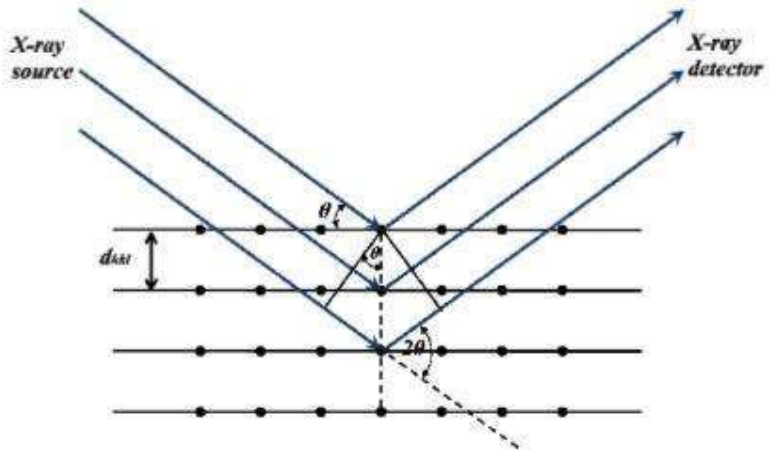

Figure 2.3: Demonstration of Bragg's Law

The diffraction satisfies the Bragg equation:

$$n\lambda = 2dsin\theta \qquad (2.1)$$

Here d is the spacing between diffracting planes, is the incident angle, n is an integer, and λ is the beam's wavelength.[8-9]

The XRD data were recorded in steps scan mode with a slow-scanning rate. The different phases were interpreted by recording an X-Ray diffraction pattern at room temperature on an X-Ray diffractometer (Rigaku Miniflex II, Japan) has Cu Kα radiation having wavelength λ= 1.5418 Å at an applied voltage of 40 kV and current of 40 mA. In this work, the XRD pattern has been recorded in the range of 10°-90° with a step size of 0.02°. The XRD setup is shown in Figure 2.4.

Figure 2.4.: Rigaku Miniflex II, Desktop XRD Setup

2.3.2 Phase Confirmation and Crystal Structure Studies by Powder X-Ray diffraction

X-ray diffraction (XRD) is a versatile, non-destructive technique that reveals detailed information about the crystallographic structure of natural and manufactured materials. X-ray radiations most commonly used are that emitted by copper, whose characteristic wavelength for the Cu-Kα radiation is a=1.5418Å. When the incident beam strikes a powder sample, diffraction occurs in every possible orientation of 2θ. The diffracted beam may be detected

using a movable detector such as a Geiger counter connected to a chart recorder. The X-ray diffraction setup is shown in Figure2.4. The counter is set to scan over a range of 2θ values at a constant angular velocity in regular use. Routinely, a 2θ range of 10 to 80 degrees is sufficient to cover the most valuable part of the powder pattern. The scanning speed of the counter is usually 2θ of 2° min^{-1}; therefore, about 30 minutes are needed to obtain a trace. Based on the principle of X-ray diffraction, a wealth of structural, physical, and chemical information about the material investigated can be obtained. A host of application techniques for various material classes are available, revealing the specific details of the sample studied.

Whether the unknown sample is single-phased or multi-phased, Phase identification is the most crucial application of X-ray diffraction studies. This identification guides us in understanding the sources of mechanisms that are taking place behind this phase formation. This also gives an idea of the correlation of crystal structure with different properties, i.e. structure-property correlation (Neumann's principle).[9]

Rietveld refinement is a widely used refinement technique for powder X-ray diffraction (XRD) based on the proposed method by Hugo Rietveld in the 1960s.[10] The Rietveld method involves fitting of a calculated profile (including all the structural and the instrumental parameters) to the experimental data. It employs the non-linear least-squares technique and requires a reasonable approximation of many free parameters in the initial stage, which includes peak shape, dimensions of the unit cell, and all the atomic coordinates in the structure of the crystal. Other parameters can be refined reasonably by guessing. In this way, refinement of crystal structure of a powder material from the PXRD data can be performed. The successful outcome of the refinement method is directly related to quality of the data, quality of the model (includes initial approximation), and the experience of the user.

A typical diffraction pattern is described by the positions, shapes, and the intensities of multiple Bragg's reflection. Each of the three properties mentioned encodes some information related to crystal structure, properties of the sample, and the properties of instrumentation.

Pattern component	Crystal structure	Specimen property	Instrumental parameter
Peak position	Unit cell parameters (a, b, c, α, β, γ)	• Absorption • Porosity	• Radiation (wavelength), • Instrument/sample alignment • Axial divergence of the beam
Peak intensity	Atomic parameters (x, y, z, B, etc.)	• Preferred orientation • Absorption • Porosity	• Geometry and configuration • Radiation (Lorentz polarization)
Peak shape	• Crystallinity • Disorder • Defects	• Grain size • Strain • Stress	• Radiation (spectral purity) • Geometry • Beam Conditioning

Table 2.1: Powder diffraction pattern as a function of various crystal structure, specimen, and instrumental parameters[11]

2.3.3 Scanning Electron Microscope

A scanning electron microscope (SEM) is a type of electron microscope that produces images of a sample by scanning it with a focused beam of electrons. A cathode in the electron gun of SEM provides a narrower beam at low and high electron energy, resulting in improved spatial resolution and minimized sample charging and damage. The field gradient in a vacuum generates the electrons. Then the beam passed through electromagnetic lenses was focused onto the specimen, resulting in the generation of various types of electrons through this interaction. A detector discovers the secondary electrons, and an image of the sample surface is formed by comparing the beam's intensities of secondary & primary electrons. The electrons interact with atoms in the sample, producing various signals that can be detected and contain information about the sample's surface topography and composition. The electron

beam is scanned in a raster scan pattern, and the beam's position is combined with the detected signal to produce an image.[12-13] The image has been recorded by EVO18, Zeiss, Japan, and set up is shown in Figure 2.5.

Figure 2.5: SEM Facilities, IIT (BHU)

2.3.4 Transmission Electron Microscopy (TEM)

In material science and engineering advancement, it is necessary to observe, analyze, and understand the phenomena occurring on a small size scale by Transmission Electron microscopy. The fine ground powder of the samples is mixed in ethanol and ultrasonicated for about 50 minutes. After proper mixing and homogenization, the sample was drop cast on a copper grid. The sample was dried in an oven at 100 °C overnight. Both diffraction and imaging mode sample was investigated. The transmission electron microscope (TEM) is a powerful and versatile instrument that permits the characterization of materials. It provides a variety of information obtained from different modes such as bright field (BF) & dark field (DF) imaging, selected area diffraction (SAD), and high-resolution lattice imaging. BF and

DF imaging are used to characterize defects and domain structures. SAD with a combination of tilting of crystal in the microscope allows reconstructing the reciprocal space and, in the way, obtaining information about the crystal structure and identifying different phases. In a TEM, a high energy (~200 keV) electron beam is transmitted through the specimen. During transmission, electrons interact with the specimen, giving rise to signals containing information about the internal structure and chemistry of the specimen. Electron diffraction patterns and lattice images are two forms of data that give an insight into crystallographic information in TEM.

Interaction of electrons with the specimen after entering the sample, most electrons are elastically scattered by the nuclei of the atoms in the specimen. Some electrons are inelastically scattered by the nuclei of the atoms in the specimen. (Figure2.6). Compared to X-ray or neutron diffraction, the interaction of electrons with the specimen is vast, and multiple scattering events are expected. For thick specimens at lower resolutions, an incoherent particle model can describe the interaction of the electrons with the specimen. The electrons passing the specimen near the nuclei are somewhat accelerated, causing a slight, local reduction in wavelength, resulting in a small phase change of electrons. Information about the specimen structure is therefore transferred to the phase of the electrons. For the formation of high-resolution images, only the elastically scattered electron is of importance. The inelastically scattered electrons contribute mainly to the background of the image. The inelastically scattered electrons also produce Kikuchi lines in the electron diffraction pattern, which is helpful for the crystal's accurate crystallographic alignment in the specimen.[14]

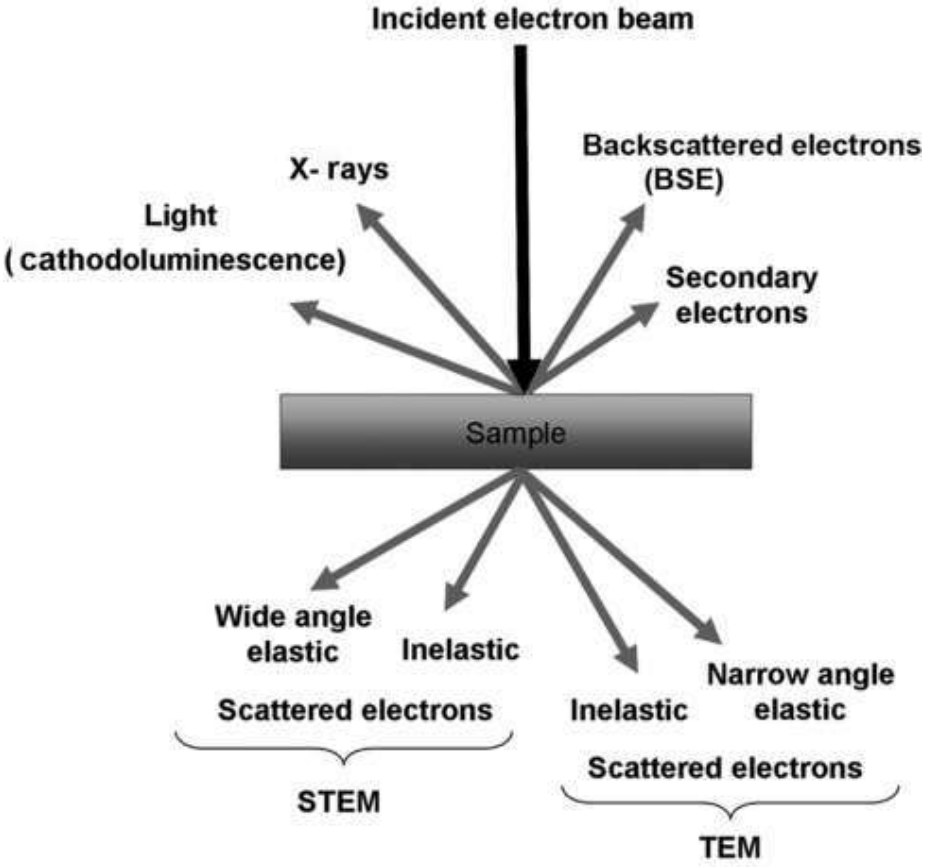

Figure 2.6: Interaction of electrons with sample [14]

2.3.5 Energy Dispersive X-Ray Spectroscopy (EDAX)

The Energy Dispersive X-Ray analysis is a non-destructive X-ray analysis to identify the elemental composition of materials. This is generally attached with structural analysis techniques such as SEM and TEM, where a high-energy electron beam & the ejected electrons from the inner shell of an atomic orbital is used to identify the specimen of interest. The resulting inner shell vacancy is filled by electrons available in the shell close to the vacant shell; these transitions are emitted as X-rays. Thus, the information corresponding to the elements of the samples can be analyzed based on the energy of emitted X-Rays. Sometimes X-Ray mapping may not show the distribution of elements that are not of interest because the characteristics X-Rays of elements of interest are close to those not desired. It

happens when the energy difference between the desired and undesired elements is equal to the spectrometer energy resolution. This method quantitatively evaluates the points on the sample while scanning the electron beam; that is why it is also called quantitative mapping of the sample. In this thesis work, we have used EDAX with SEM and TEM to study the electron mapping of the composition. Figure 2.5 & 2.7 show the SEM & TEM setup attached with EDAX sprectrometer.[15]

Figure 2.7: TEM Facilities with EDAX spectrometer, IIT (BHU)

2.3.6 BET (Brunner-Emmett-Teller theory) surface area measurement

BET determines the specific surface area and pore size distribution of the material. Those surface areas will further assist to understand the catalytic activity, moisture retention, and shelf life. BET utilizes the physical adsorption of gas (nitrogen gas) on the surface of a solid to determine its specific surface area. Physical adsorption involves van der Waals force between adsorbate and adsorbent. After adsorption of gases desorption will occur. Hence the

amount of adsorption of a gas on the adsorbent will determine the required specific surface area of the sample. BET process is usually carried out at constant temperature or under the isothermal condition which was maintained by liquid nitrogen. On the other side, the pressure or the concentration of the adsorbate gas kept on increasing. Therefore graph has been plotted between the relative pressure of the gas and volume adsorbed onto the sample.[16-17]

BET is carried out in three-step:

1. Standardisation of the reference cell.

2. Pre-treatment of the sample by heating at a specific temperature.

3. Adsorption of adsorbate onto the adsorbent under isotherm conditions.

Figure 2.8: BET (Brunner-Emmett-Teller theory), CIFC. IIT(BHU)

2.3.7 Thermogravimetric analysis (TGA)

The TGA analysis is a technique used to determine the thermal stability of the materials. In this method, the mass of the sample is recorded as a function of temperature, which is used to take information about the change in mass (absorption or desorption), phase transition, and thermal decomposition. If the mass of the sample remains constant in a given temperature

range, then the sample is said to be thermally stable in that range. TGA also helps determine the calcination temperature of the sample as it provides the upper limit of temperature beyond which degradation of the sample starts.

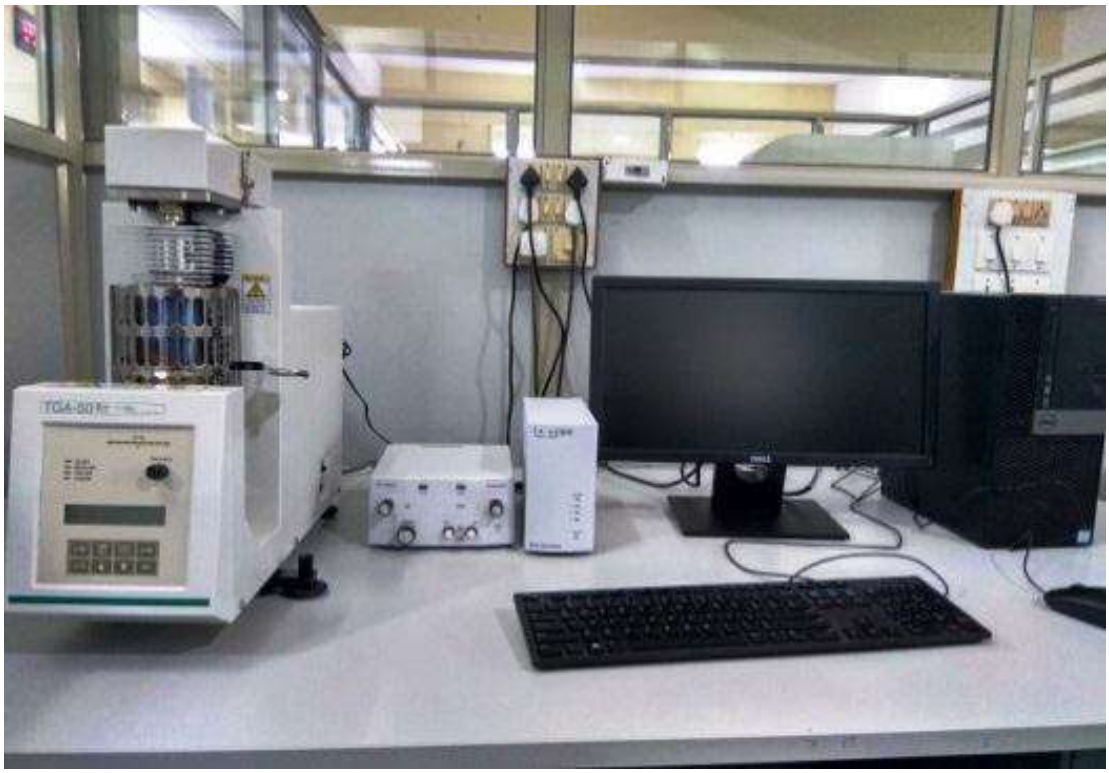

Figure 2.9: TGA, IIT (BHU)

2.3.8 Differential Scanning Calorimetry(DSC)

Differential scanning calorimetry (DSC) is a thermos analytical technique to analyze any thermal behavior change during the phase transition within the system. In this technique, heating or cooling of a test sample and an inert reference sample is done under identical conditions. The difference in the amount of heat required to increase the temperature of the test sample and reference sample to maintain them both at the same temperature is recorded. In this technique, the material under consideration is placed in fine powder in a tiny capsule that is often of alumina or other suitable refractory material. Along with this test sample, a second capsule containing an inert powder such as α-Al2O3, which does not exhibit

endothermic or exothermic effects, is placed. Thermocouples are embedded in the test substance and the α-Al2O3 powder and are connected. Therefore, their electromotive forces are opposed; the net electromotive forces represent the temperature difference between the sample powder and the inert α-Al2O3. The two capsules are heated at a constant rate, and the temperature difference is plotted either against time or against the temperature at some fixed points within the apparatus. Any physical or chemical change occurring to the test sample, which involves the evolution of heat, will cause its temperature to rise temporarily above the reference sample leading to an exothermic peak.

Conversely, a process accompanied by the absorption of heat will cause the temperature of the test sample to lag behind that of the reference sample, leading to an endothermic peak. The area under any given peak can be used as a quantitative measure of the amount of heat evolved or absorbed by the physical or chemical changes. The Combined study of TGA/DSC also gives an idea about the reaction pathway for the prepared mixture of raw materials and various transition points such as melting point, glass transition temperature, crystalline temperature, etc. In this thesis work, TGA & DSC has been carried on multiple samples in the temperature range of 30°C to 800°C in a nitrogen gas atmosphere.[18]

Figure 2.10: DSC, CIFC. IIT(BHU)

2.3.9 FTIR Spectroscopy

Infrared Spectroscopy is an important technique for the analysis of materials that provides the fingerprint of the samples. The absorption of FTIR peaks corresponds to the frequencies of vibrations between the bonds of the atoms which are responsible for building up the materials. Since each material possesses a unique combination of atoms so no two compounds produce the same infrared spectrum. This thesis work uses a Thermo Scientific Nicolet iS5 FTIR spectrometer and data were recorded within 400-4000 cm^{-1}. In FTIR, the beam of light of different frequencies interacts with the sample which excites and vibrates the covalent bond containing dipole moments, and the detector detects the intensity of light after the interaction. To determine the amount of light absorbed at each wavelength, the interferogram is subjected to Fourier transform. The data set can be collected in reflected,

absorbed, or transmitted mode. The energy consumed by the bonds is determined by the types of bonds present, thus characteristic spectrum was obtained.[19]

Figure 2.11: FTIR Spectrometer, CIFC. IIT(BHU)

2.3.10 X-ray photoelectron spectroscopy (XPS)

X-ray photoelectron spectroscopy (XPS) is a technique providing surface compositional information, electronic states, bond type, and valence of the elements. To perform XPS, the sample is bombarded with a beam of X-rays that has a narrow energy range. These X-rays are absorbed by the electrons associated with the atoms in the sample and some of the electrons are then ejected from the sample surface; the electrons are called photoelectrons. Photoelectrons are low energy and their escape depth is about 10 nm (near the surface region of a sample). The energy of the ejected electrons is measured and this gives information on the atomic species and the types of 46 bonds present in the sample. Based on the law of energy conservation, photoemission is described by the following equation: $E_k = h\nu - E_B$ where h is the Planck's constant, v is the frequency of the X-ray photon, Ek is the kinetic

energy measured by the electron energy analyzer scanning the kinetic energy spectrum and EB represents the electron binding energy of the i-th level. By counting the number of electrons at different binding energies, an energy spectrum can be precisely produced via a pattern with intensity vs binding energy. The specific binding energy of the electron acts as the blueprint to identify the composition of the sample with the intensity corresponding to the quantity of the element. High resolution (HR)-XPS can be achieved using an additional monochromator in the XPS system to reduce energy width dispersion. Additionally, lower spectral background and the elimination of unwanted X-rays can also be accomplished. The detection limit for the XPS is usually in the parts per thousand range. However, higher resolution can be obtained with extended signal collection time. [20]

Figure 2.12: X-ray photoelectron spectroscopy (XPS), CIFC. IIT(BHU)

2.3.11 Electrochemical Measurements

Electrochemical measurements are used to measure the electrochemical performance of the electrode prepared for the supercapacitor. Three major techniques are used to measure electrochemical performance: cyclic voltammetry (CV), galvanostatic charge-discharge (GCD), and electrochemical infrared spectroscopy (EIS).

2.3.11.1 Cyclic Voltammetry (CV)

Cyclic voltammetry (CV) is the most used characterization technique in analytical chemistry for the investigation of thermodynamics in a redox reaction, electron transfer reaction kinetics, and identification of substrate adsorption behavior on electrode while in the case of electrochemistry it is used to study redox reaction behavior and measurement of specific capacitance and stability of electrode material. Voltammograms are the curve of potential window versus current density and which are obtained by measuring the current at the working electrode at a continuous potential scan.

The three-electrode system is the basic arrangement of the cell to understand the electrochemical behavior of the sample. Three electrode systems consist of a working electrode (WE) and counter electrode (CE) and reference electrode (RE). Potentiostat will control the potential between WE and CE, while it measures the potential difference between WE and RE. As a galvanostat, the instrument controls the current between WE and CE. The potential difference of WE with respect to RE and the current flowing between the CE and WE are continuously analyzed by the software called NOVA1.1. Therefore, as earlier mentioned the graph plotted between specific current and the potential difference is called "Cyclic Voltammeter".[21]

The working electrode is an electrode over which the reaction of interest is occurring. Mostly glassy carbon, graphite sheet, and carbon paper can be used as a current collector over which active material/working electrode has been coated. The counter electrode exhibits inert behavior such as Platinum, gold, graphite, and glassy carbon which generally doesn't involve in the electrochemical reaction. The current circuit of the electrochemical cell has been closed using these counter electrodes. Reference electrodes are those electrodes whose electrode potentials are well known such as Ag/AgCl and saturated calomel electrode (SCE).

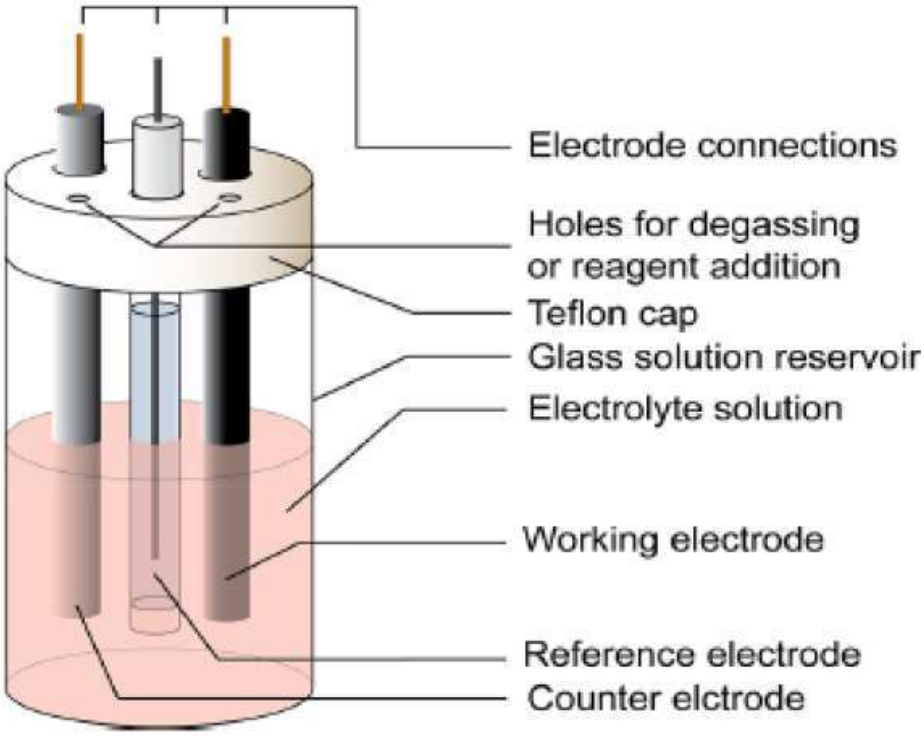

Figure. 2.13: Conventional three electrodes setup used in electrochemical testing

2.3.11.2 Galvanostatic Charge-Discharge (GCD)

Similarly the cyclic voltammetry technique, GCD technique is used for measurement of electrochemical performance of supercapacitor electrode through charge and discharge cycle in a controlled current condition. In the GCD technique, the current is controlled and voltage is measured where the current pulse is applied for the working electrode and the resulting voltage is noted against the reference electrode with respect to the time function. When current is applied, due to internal resistance measured potential changes abruptly, after that it changes gradually due to over-potential developed across electrode as the concentration of the reactant is exhausted at the electrode surface.[22] Using GCD the parameters such as specific capacitance, resistance and cyclability can be calculated. The voltage equation for GCD is given below:

$$(t) = iR + \frac{t}{c} i(V) \qquad (2.2)$$

From the charge-discharge curve, the specific capacitance of the electrode can be calculated as:

$$C_{sp} = \frac{I\Delta t}{m\Delta V} \qquad (2.3)$$

2.3.11.3 Electrochemical Impedance Spectroscopy (EIS)

EIS measurement was conducted to understand the cyclic capacity or capacitance fading in case of pseudocapacitance From EIS measurement the graph has been plotted between imaginary impedance ($Z_{imaginary}$) at the y-axis and real impedance (Z_{real}) at the x-axis termed as "Nyquist plot". Generally, EIS measurement displays a semicircle in the high-frequency range to the low-frequency range. In this work, the electrochemical stability test performed AC EIS measurements shown in the Nyquist plot at OCP in the frequency range (1 MHz to 0.1 Hz). The specific impedance contribution is mainly attributed to the impedance distributions over electric series resistance (R_s), charge transfer resistance (R_{ct}), and Warburg impedance (R_w). At higher frequency, the intercept in the EIS spectra on the real axis indicates very small internal resistance. The small semicircle in the high-frequency region also shows the fast charge transport between electrode and electrolyte. Lower frequency data represent the Warburg diffusion resistance, the straight line in the low-frequency region is close to 90° angle (very close to -Z"(Ω) axis) from the horizontal line represents the characteristic of pseudo capacitance behavior. This also represents fast ion diffusion in the porous structure.[22]

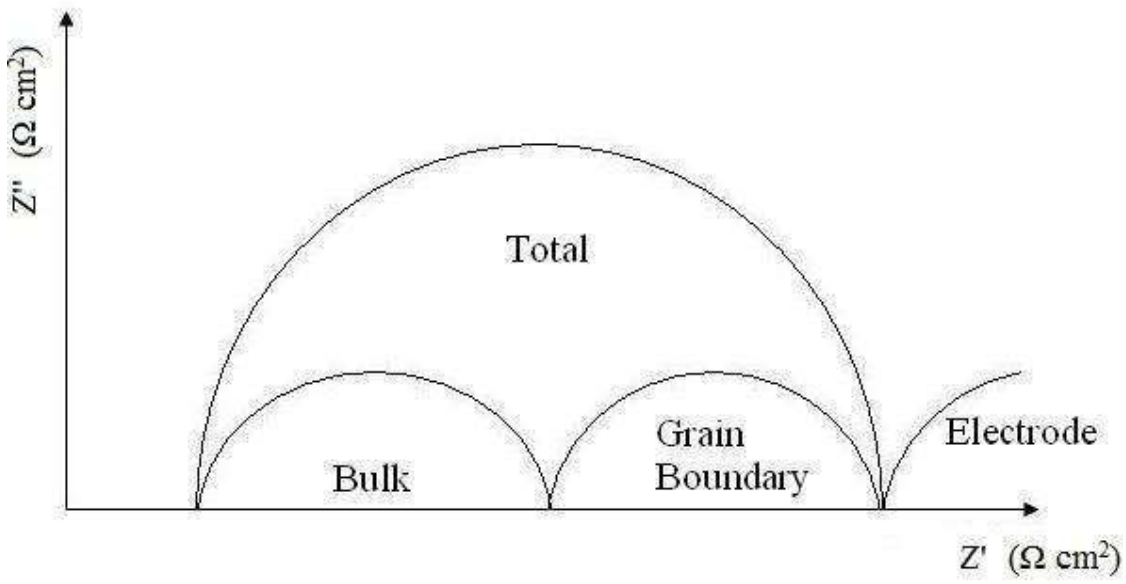

Figure 2.14 Nyquist Plot for ionic solids (Z" = imaginary impedance, Z' = real impedance) [8].

2.3.11.4 Chemical Kinetic of pseudocapacitors from Cyclic voltammetry curve

The type of supercapacitor can be distinguished by Current-Voltage response, This section discusses the kinetics of pseudocapacitance by cyclic voltammetry polarization curve,

1. Linear or pseudo linear relationship between the applied potential and state of charge (capacitance, dQ/dV)

2. Nearly ideal electrochemical reversibility

3. Surface-controlled kinetics

Lindström et al. Studied kinetics of Li^+ insertion into nano, porous anatase TiO_2 films and they found a relationship between the applied sweep rate and observed electrochemical current, they introduced b-value analysis. b value determines the presence of surface controlled/ capacitive (vs. semi-infinite diffusion-controlled) kinetics:[23]

$$i(V) = av^b \qquad (2.4)$$

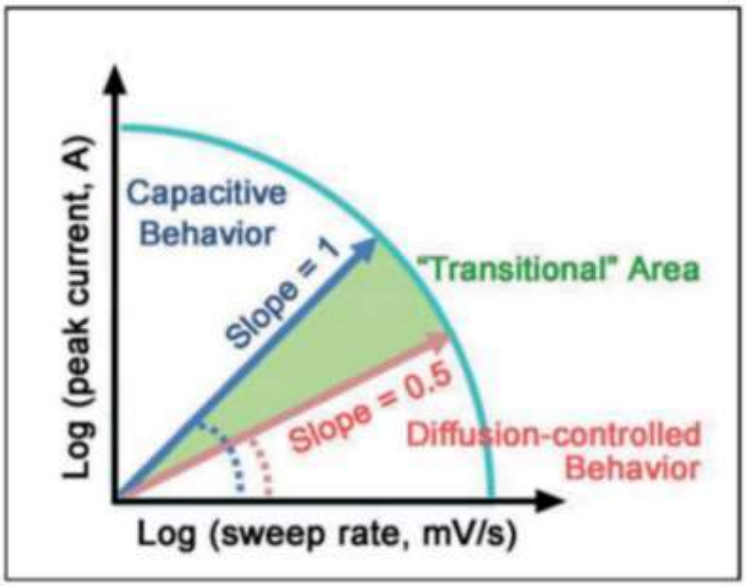

Figure 2.15 Power-law dependence of the peak current on sweep rate for capacitive materials (b= 1.0) and typical battery-type materials (b = 0.5). The "transition" area between capacitive and battery-type materials area is located in the range of b = 0.5–1.0. [23]

Where i(V) is the current at a specific potential, sweep rates ν. a and b are adjustable parameters, and the b value can be determined as the slope of log(i) vs log(ν) for various sweep rates. When b = 1 is denoted surface control and 0.5 denoted diffusion control. When the b-value falls between 0.5 and 1, the mechanism is attributed to a combination of diffusion and capacitive contributions b value presentation shown in Figure 2.15.

Liu et al. proposed a linear combination of surface- and diffusion-controlled currents [24]

$$i(V) = k_1(V)\,\nu + k_2(V)\,\nu^{1/2} \qquad (2.5)$$

Dunn et al. utilized this concept to deconvolute capacitive vs diffusive contributions to the total current for many types of nanostructured transition metal oxides. [25-27]

$$i(V)/\nu^{1/2} = k_1(V)\,\nu^{1/2} + k_2(V) \qquad (2.6)$$

k_1 and k_2 determine surface and diffusion-controlled processes at specific potentials with multiple sweep rates. The method allows for the separation of the cyclic voltammograms into surface-controlled and diffusion-controlled regions.

Trasatti et al. developed another new method based on voltammetric charge to deconvolute the "inner" (less accessible) and "outer" (more accessible) surface contributions.[28]

According to Trasatti, voltammetric charge (Q) can be divided into surface-controlled and diffusion-controlled contributions,

$$Q = Qs + Qd \qquad (2.7)$$

Where Qs and Qd are the surface-controlled and diffusion-controlled contributions to charge, respectively. Surface-controlled charge contribution also be divided into the "inner" surface contribution, Qs, in, and "outer" surface contribution,

$$Qs = Qs, in + Qs, out \qquad (2.8)$$

The "inner" surface contribution is sweep rate dependent (due to lower accessibility of redox sites) and the outer" surface contribution is invariant of sweep rate, Assuming semi-infinite linear diffusion and a linear relationship between Q_d and $\nu^{-1/2}$, equation (2.8) can be rearranged to determine Qs, out when

$$Q = Q_{s,\,out} A1 = + \nu^{-1/2} \qquad (2.9)$$

Where A1 is a constant. The y-intercept ($\nu^{-1/2} = 0$; or $\nu = \infty$) determines Qs. On the other hand, Qs is determined when $\nu = 0$. Assuming Q^{-1} decreases linearly with $\nu^{1/2}$, equation 2.9 is rewritten as

$$Q^{-1} = Q_s^{-1} A_2 \nu^{1/2} \qquad (2.10)$$

Where A_2 is another constant. Qs^{-1} can be obtained from the y-intercept ($\nu 1/2 = 0$)

References

1. L. Merabet, K. Rida, N. Boukmouche, Sol-Gel Synthesis, Characterization, and Supercapacitor Applications of MCo_2O_4 (M=Ni, Mn, Cu, Zn) Cobaltite Spinels, *Ceramics International*, 44 (2018) 11265.
2. G. Yang, S. J. Park, Facile Hydrothermal Synthesis of $NiCo_2O_4$-Decorated Carbon as Electrodes for High Performance Asymmetric Supercapacitors, *Electrochim. Acta*, 285 (2018) 405.
3. C. Lamiel, V. H. Nguyen, C. Roh, C. Kang, J. J. Shim, Synthesis of Mesoporous RGO@$(Co,Mn)_3O_4$ Nanocompositeby Microwave-Assisted Method for Supercapacitor Application, *Electrochim. Acta*, 210 (2016) 240.
4. W. Mi, C. Dai, S. Zhou, J. Yang, Q. Li, Q. Xu, Chemical Precipitation Synthesis of KCoF3 for Supercapacitor Applications, *Mater. Lett*., 227 (2018) 66.
5. H. Xin, Z. Xu, Y. Liu, W. Li, Z. Hu, 3D Flower-Like NiCo2O4 Electrode Material Prepared by a Modified Solvothermal Method for Supercapacitor, *J. alloys Compds*., 711 (2017) 670.54
6. Z. B. Jao, J. H. Luan, M. K. Miller, Y. W. Chung, C. T. Liu, Co-Precipitation of Nanoscale Particles in Steels with Ultra-High Strength for a New Era, *Materials Today*, 20 (2017) 142.
7. A. Bitar, C. Kaewsaneha, M.M. Eissa, T. Jamshaid, P. Tangboriboonrat, D. Polpanich, A. Elaissari, Ferrofluids: from preparation to biomedical applications, J. Colloid Sci. Biotechnol. 3 (2014) 3–18.
8. Borie, B. X-Ray Diffraction in Crystals, Imperfect Crystals, and Amorphous Bodies. Journal of the American Chemical Society. 1965, pp 140–141.
9. B. D Cullity, Elements of X- Ray Diffraction

10. Rietveld, H. M. (2 June 1969). "A profile refinement method for nuclear and magnetic structures". Journal of Applied Crystallography. 2 (2): 65–71.
11. Pecharsky, V. K., & Zavalij, P. Y. (2009). Fundamentals of Powder Diffraction and Structural Characterization of Materials
12. Lott, P. F. Handbook of Microscopy; 1985; Vol. 31.
13. Amelinckx, S.; van Dyck, D.; van Landuyt, J.; van Tendeloo, G. Handbook of Microscopy: Applications in Materials Science , Solid-State Physics and Chemistry; 2008.
14. David B. Williams and C. Barry Carter Transmission electron microscopy, (Plenum, 1996)
15. EDAX: https://en.wikipedia.org/wiki/Energy-dispersive_X-ray_spectroscopy.
16. Sing, K. S. Adsorption methods for the characterization of porous materials. Advances in Colloid and Interface Science, 1998, 76, 3-11.
17. Donohue, M. D.; Aranovich, G. L., Classification of Gibbs Adsorption Isotherms. Adv. Colloid Interface Sci. 1998, 76, 137-152..
18. M.E.Brown , Introduction to thermal analysis : Techniques and application , second edition, Springer, 2007.
19. B. Stuart, Spectral analysis. Infrared spectroscopy: fundamentals and applications, (2004).45-70.
20. P. Van der Heide, X-ray photoelectron spectroscopy: an introduction to principles and practices. John Wiley & Sons
21. N. Elgrishi, K.J. Rountree, B.D. McCarthy, E.S. Rountree, T.T. Eisenhart, J.L. Dempsey, A Practical Beginner's Guide to Cyclic Voltammetry, J. Chem. Educ. 95 (2018) 197–206.

22. A. J. Bard, & L. R. Faulkner, Fundamentals and applications. Electrochemical Methods, 2001, 2, 482.

23. Liu, T.-C.; Pell, W. G.; Conway, B. E.; Roberson, S. L. Behavior of Molybdenum Nitrides as Materials for Electrochemical Capacitors Comparison with Ruthenium Oxide. J. Electrochem. Soc. 1998, 145, 1882−1888

24. Brezesinski, T.; Wang, J.; Polleux, J.; Dunn, B.; Tolbert, S. H. Templated Nanocrystal-Based Porous TiO_2 Films for next-Generation Electrochemical Capacitors. J. Am. Chem. Soc. 2009, 131, 1802−1809

25. Brezesinski, T.; Wang, J.; Senter, R.; Brezesinski, K.; Dunn, B.; Tolbert, S. H. On the Correlation between Mechanical Flexibility, Nanoscale Structure, and Charge Storage in Periodic Mesoporous CeO_2 Thin Films. ACS Nano 2010, 4, 967−977.

26. Brezesinski, K.; Wang, J.; Haetge, J.; Reitz, C.; Steinmueller, S. O.; Tolbert, S. H.; Smarsly, B. M.; Dunn, B.; Brezesinski, T. Pseudocapacitive Contributions to Charge Storage in Highly Ordered Mesoporous Group v Transition Metal Oxides with Iso-Oriented Layered Nanocrystalline Domains. J. Am. Chem. Soc. 2010, 132, 6982−6990.

27. Ardizzone, S.; Fregonara, G.; Trasatti, S. Inner" and "Outer" Active Surface of RuO2 Electrodes. Electrochim. Acta 1990, 35, 263−267

28. Zheng, J. P.; Cygan, P. J.; Jow, T. R. Hydrous Ruthenium Oxide as an Electrode Material for Electrochemical Capacitors. J. Electrochem. Soc. 1995, 142, 2699−2703

.